Published in final edited form as:
Cancer Discov. 2013 August ; 3(8): 908–921. doi:10.1158/2159-8290.CD-12-0507.

PTEN-null Tumors Cohabiting the Same Lung Display Differential Akt Activation and Sensitivity to Dietary Restriction

Natasha L. Curry[1], **Mari Mino-Kenudson**[3], **Trudy G. Oliver**[4], **Ömer H. Yilmaz**[3,6], **Vedat O. Yilmaz**[1], **Jade Y. Moon**[1], **Tyler Jacks**[4], **David M. Sabatini**[4,5,6], and **Nada Y. Kalaany**[1,2]

[1]Division of Endocrinology, Center for Basic and Translational Obesity Research, Boston Children's Hospital, Boston, MA 02115

[2]Department of Pediatrics, Harvard Medical School, Boston, MA 02115

[3]Department of Pathology, Massachusetts General Hospital and Harvard Medical School, Boston, MA 02114

[4]Howard Hughes Medical Institute and Department of Biology, Massachusetts Institute of Technology; The David H. Koch Institute for Integrative Cancer Research at MIT, Cambridge, MA 02139

[5]Broad Institute of Harvard and MIT, Cambridge, MA 02142

[6]Whitehead Institute for Biomedical Research, Cambridge, MA 02142

Abstract

PTEN loss is considered a biomarker for activated PI3K/Akt, a pathway frequently mutated in cancer, and recently shown to confer resistance to dietary restriction (DR). Here we demonstrate that *PTEN* loss is not sufficient to drive Akt activation and resistance to DR in tumors with low growth factor receptor levels. We describe a murine *PTEN*-null *Kras*-driven lung cancer model that harbors both DR-resistant, higher-grade, bronchiolar tumors with high-Akt-activity, and DR-sensitive, lower-grade, alveolar tumors with low-Akt-activity. We find that this phenotype is cell-autonomous and that normal bronchiolar cells express higher levels of IGF1R and ENTPD5, an endoplasmic reticulum (ER) enzyme known to modulate growth factor receptor levels. Suppression of *ENTPD5* is sufficient to decrease IGF1R levels and sensitize bronchiolar tumor cells to serum *in vitro* and to DR *in vivo*. Furthermore, we find that a significant percentage of human non-small cell lung cancer (NSCLC) have low Akt activity despite *PTEN* loss.

Keywords

Lung cancer; *PTEN* loss; ENTPD5; PI3K/Akt; dietary restriction

Corresponding Author: Nada Y. Kalaany, Division of Endocrinology, Center for Basic and Translational Obesity Research, Boston Children's Hospital and Harvard Medical School, Boston, MA 02115. Phone: 617-919-4896; Fax: 617-730-0856; nada.kalaany@childrens.harvard.edu.

Note: T.G. Oliver present address: Department of Oncological Sciences, University of Utah and Huntsman Cancer Institute, Salt Lake City, UT 84112

Disclosure of Potential Conflict of Interest No potential conflicts of interest were disclosed.

Author Contributions N.Y.K. and D.M.S. conceived the project and N.Y.K. designed experiments. N.C. and N.Y.K. performed, and V.O.Y and J.Y.M. assisted with experiments. O.H.Y. assisted with FACS analysis. T.J. suggested using the lung cancer mouse models and T.G.O generated and provided the KPTEN and Kp53 mice; M.M.-K. assisted with analysis of human tissue immunohistochemistry and pathology. N.Y.K. wrote and D.M.S. edited the manuscript.

Introduction

DR has long been known to have anti-tumorigenic effects (1). We recently showed however, that tumors with activated phosphatidylinositol-3 kinase (PI3K) pathway are resistant to DR (2). PI3K is a lipid kinase whose activation through binding of insulin/insulin-like growth factor-1 (IGF1) to receptor tyrosine kinases leads to the recruitment and activation of Akt (3). In turn, Akt, a serine/threonine kinase that is aberrantly activated in a multitude of cancers, enhances cellular growth and inhibits apoptosis. This signaling cascade is antagonized by the lipid phosphatase activity of the tumor suppressor phosphatase and tensin homologue (PTEN) (4, 5). Genetic loss of *PTEN* has been considered a predictive biomarker of Akt activation and response to therapies in different cancers (6, 7).

Using various human xenograft and genetically engineered mouse models of cancers of different tissues, we have previously shown that tumors with PI3K activation resulting from either activating mutations in PI3K catalytic subunit (*PIK3CA*) or *PTEN* loss are resistant to DR (2). However, the question of whether PI3K-driven versus non-PI3K-driven tumors of the same tissue, in an otherwise genetically identical host, would display differential sensitivities to DR, remains unanswered. Here, we investigate the response of lung tumors to DR, using two *Kras*- driven mouse models of lung cancer with either loss of the tumor suppressor *p53*, or alternatively, loss of *PTEN*. We demonstrate that adjacent tumors cohabiting the same lung can have differential Akt activities and sensitivities to DR, despite *PTEN* loss. Such heterogeneity is contingent upon the expression of the ER enzyme, ENTPD5, which modulates growth factor receptor levels in cells with active Akt (8).

Results

Adjacent *PTEN*-null, *Kras*-driven Lung Tumors Display Differential Akt Activation and Sensitivity to DR

In order to investigate the responses of PI3K-driven and non-PI3K-driven tumors of the same tissue to DR, we utilized two conditional genetically engineered mouse models of lung cancer: $LSL\text{-}Kras^{G12D};p53^{fl/fl}$ (9, 10) and $LSL\text{-}Kras^{G12D};PTEN^{fl/fl}$ (9, 11) (hereafter referred to as Kp53 and KPTEN models, respectively). Upon administration of adenoviral-Cre recombinase through nasal inhalation, both models develop lung cancer that is respectively driven by Kras activation plus loss of the tumor suppressor *p53* (Kp53 mice), or alternatively by Kras activation and *PTEN* loss (KPTEN mice). Although both Kp53 and KPTEN mice develop adenomas at full penetrance following Cre-mediated recombination, KPTEN (12) tumors grow at a higher rate than Kp53 (13) tumors, causing death at an earlier time-point. Therefore, we waited either 1 week (KPTEN mice), or 6 weeks (Kp53 mice) post-infection so as to reach a comparable tumor burden, prior to subjecting these mice to a dietary regimen.

Both mouse models were subjected to *ad-libitum* feeding or DR (2) (40%) for 3 weeks, at which point the tumor response to the different diets was analyzed. All mice experienced similar decreases in body weight (25%), and lower plasma insulin and IGF1 levels at the end of the restriction period, independent of genotype (Supplementary Fig. S1A-S1C). Unexpectedly however, the tumor burden upon DR was decreased, to a similar extent, in both KPTEN and Kp53 mice (3.6-fold and 4.5-fold, respectively) (Fig. 1A and Supplementary Fig. S1D). Because the KPTEN tumors did not display resistance to DR, we further investigated whether Akt was indeed activated in these tumors. Careful histological and immunohistochemical examination of the lung sections from these mice (Fig. 2A and B and Supplementary Fig. S2A) revealed the presence of two adjacent types of tumors in both KPTEN and Kp53 models: lower-grade adenomas (hereafter referred to as alveolar tumors) that express the alveolar marker surfactant protein c (SPC) (14); and higher-grade, atypical

papillary tumors, localized to the bronchioles. Both alveolar and bronchiolar tumors of the Kp53 mouse, similar to wild-type cells, had low to undetectable Akt activity levels (Fig. 2C, middle and right panels), which correlated with *PTEN* expression (Fig. 2D, middle and right panels). Interestingly however, the KPTEN mouse displayed differential Akt activation in the different types of tumors: whereas bronchiolar tumors have significant Akt activation, adjacent alveolar tumors maintain low to undetectable Akt activity (Fig. 2C, left panels). To investigate the possibility that *PTEN* was differentially lost in bronchiolar but not alveolar tumors of the KPTEN mouse, we performed immunohistochemical analysis on sequential lung sections and found that *PTEN* was indeed deleted in both types of tumors despite their differential Akt activation (Fig. 2D left panels). These results were confirmed at the genetic level, using laser capture microdissection (data not shown). Indeed, compared to Kp53 lungs where *PTEN* presence was noted in all cells, KPTEN lungs only displayed *PTEN* expression in normal tissue, endothelial cells and CD68-positive macrophages that are dispersed within the tumors (Fig. 2D and Supplementary Figs. S2B, S2C, S3A and S3B).

We then investigated the cellular localization, in both Kp53 and KPTEN tumors, of the transcription factor FOXO1, whose phosphorylation by active Akt results in its exclusion from the nucleus (15). Consistent with differential Akt activity in the different tumors, we found indeed that FOXO1 was cytoplasmic in bronchiolar KPTEN tumors, independent of diet (Supplementary Fig. S4A right), but could be detected in both the nucleus and cytoplasm of KPTEN alveolar tumors and in all Kp53 tumors under *ad-libitum* and DR conditions (Supplementary Fig. S4A left, and S4B).

The observed differential Akt activation in KPTEN mice led us to re-investigate the tumor burden response to DR, taking into consideration the two types of tumors. We found that, in response to DR, both alveolar and bronchiolar Kp53 tumors displayed a significant decrease in total burden (~3.5-fold) (Fig. 1B). Such a decrease was represented by decreases in both the average size and number of individual alveolar tumors (56% and 57%, respectively) and bronchiolar tumors (70% and 40%, respectively) in the Kp53 lungs (Fig. 1C). In KPTEN mice however, we observed a differential tumor response to DR: whereas alveolar tumors displayed pronounced sensitivity to DR (7.4-fold decrease in total tumor burden, Fig. 1D) corresponding to 79% and 63% decreases in the average size and number of individual tumors, respectively (Fig. 1E), bronchiolar tumors were strongly DR-resistant, showing no decreases in tumor burden (Fig. 1D and E) in restricted mice. Consistently, Kp53 alveolar and bronchiolar tumors displayed a 40- 50% decrease in tumor cell proliferation upon DR, as quantified by BrdU labeling of mitotic cells. Whereas cellular proliferation in KPTEN alveolar tumors was similarly decreased (40%) under DR conditions, that of KPTEN bronchiolar tumors was not altered (Fig. 1F). Furthermore, no apoptosis (caspase-3 cleavage) was detected in tumors of either mouse model, under *ad-libitum* or DR conditions (data not shown).

The Alveolar Tumor Phenotype of Low Akt Activity Despite *PTEN* Loss is Cell-Autonomous

The observed phenotype of differential Akt activation and sensitivity to DR, despite *PTEN* loss, in adjacent tumors cohabiting the lungs of the same host, was quite surprising. We reasoned that the underlying mechanism could be either the result of a tumor-environment interaction, or alternatively, a cell-autonomous characteristic of the alveolar but not bronchiolar cells, that prevented enhanced Akt activation upon *PTEN* loss. In order to test these hypotheses, we decided to perform a syngeneic transplant experiment and ask whether this phenotype would be maintained upon changing the environment of tumors harvested from the lungs of a donor mouse to the subcutaneous region of a recipient mouse of the same strain. In order to accomplish this experiment, deletion of *p53* in the KPTEN tumor cells was necessary to overcome oncogene-induced senescence (16, 17), and to allow

subcutaneous tumor growth in the recipient mice. To that end, we incorporated the *p53*$^{fl/fl}$ allele into KPTEN mice and generated KPTENp53 mice (*LSL-Kras*^{G12D};*PTEN*$^{fl/fl}$;*p53* $^{fl/fl}$), in which *p53* would be concomitantly lost upon tumor induction. The phenotype of differential Akt activation and sensitivity to DR in adjacent alveolar and bronchiolar tumors was recapitulated in KPTENp53 mice (Supplementary Fig. S5A-S5E). Dissociated tumor cell mixtures (10^6 cells) from donor KPTENp53 mice were able to grow and form *PTEN*-null tumors (~550 mm^3 in volume) 5 weeks following their injection under the skin of a recipient mouse of the same strain (Fig. 3A and B). PTEN-positive stroma was noted in *PTEN*-null recipient tumors (Fig. 3B). We also noticed that the predominant cell population in the recipient mouse tumors was SPC-negative (bronchiolar). Importantly however, the SPC-positive (alveolar)/low Akt activity versus SPC-negative (bronchiolar)/high Akt activity phenotype of the KPTEN tumors was conserved upon transplantation and despite alteration of the tumor environment from donor to recipient mice (Fig. 3). As a control, subcutaneous transplantation of Kp53 alveolar/bronchiolar tumor mixtures in mice of the same strain showed maintenance of low Akt activity in the recipient mice (Supplementary Fig. S6A and S6B). These results implied the existence of an intrinsic characteristic of the alveolar tumor cell type, resulting in low Akt activity, despite *PTEN* loss.

ENTPD5 Expression Modulates IGF1R Levels and Sensitivity to DR in murine *PTEN*-null Lung Tumors

The cell-autonomous nature of this phenotype led us to ask whether proteins involved in the PTEN/PI3K pathway are differentially expressed in alveolar and bronchiolar tumors of the KPTEN lungs. We found that the ectonucleoside triphosphate diphosphohydrolase 5 protein (*ENTPD5*) is expressed at significantly higher levels in the bronchioles, compared to the alveoli, of normal mouse lung (Fig. 2E, right panel). ENTPD5 is an ER UDPase (18) whose activity promotes N-glycosylation and folding of proteins in the ER, including receptor tyrosine kinases (8). *ENTPD5* knockdown in *PTEN*-null cells results in ER stress, loss of growth factor receptors (e.g. IGF1R, Her-2/ErbB-2 and EGFR) and induction of apoptosis (8). Furthermore, *ENTPD5* is a target of the PI3K/Akt pathway: its expression can be suppressed by FOXO1-4 transcription factors (8), whose activity is negatively regulated by Akt (15). We find that compared to normal alveolar cells, alveolar tumors express moderate levels of ENTPD5, as detected by immunohistochemistry in KPTEN and Kp53 mice. However, a consistent, markedly higher level of ENTPD5 expression was observed in bronchiolar versus alveolar tumors in both mouse models (Fig. 2E, left and middle panels). Similarly, we find that the IGF1 receptor (IGF1Rβ) is differentially expressed in the lung, with high expression and membranous localization in normal bronchioles, as well as KPTEN and Kp53 bronchiolar tumors, but low to undetectable levels in alveolar cells (Fig. 2F). Because Akt is not equally activated in alveolar and bronchiolar tumors of KPTEN lungs despite *PTEN* loss, we hypothesize that loss of this major PI3K antagonist is not sufficient to drive Akt activation, but that additional positive upstream pathway activation is required. Differential growth factor receptor expression in the different types of cells, possibly resulting from differential *ENTPD5* expression (8), might explain such a phenotype.

To investigate this possibility, we first attempted to generate alveolar and bronchiolar tumor cell lines for *in vitro* manipulation. Because specific alveolar/bronchiolar antibodies did not allow for successful fluorescence-activated cell sorting (FACS) of tumor cell mixtures, we resorted to colony isolation in tissue culture dishes. Dissociated tumor cells from KPTENp53 lungs were seeded, at very low dilution and distinct colonies with different epithelial morphologies (Fig. 4A) were individually trypsinized, using cloning cylinders, and grown separately as cell lines. *PTEN* was confirmed to be completely lost in all isolated tumor cells, but was expressed in a control NSCLC cell line (PC-9, Fig. 4B). Expression of

the alveolar marker SPC (14) was then used to identify SPC-high (alveolar) and SPC-low (bronchiolar), tumor cells (Fig. 4B). The epithelial nature of the alveolar and bronchiolar tumor cells was further confirmed by FACS analysis using an antibody against the pan-epithelial marker EpCAM. We noted significant epithelial enrichment in both alveolar and bronchiolar cell lines, where over 88% of cells express high levels of EpCAM ($EpCAM^{hi}$) and only 0.3-1.1% express low EpCAM levels ($EpCAM^{lo}$). This is in contrast to the parental mixture, where only 11% of cells are $EpCAM^{hi}$ and the majority (~85%) of cells are $EpCAM^{lo}$ (Supplementary Fig. S7). Unfortunately, growth of alveolar tumor cells in culture resulted in higher *ENTPD5* expression levels than those observed in bronchiolar cells, enhanced Akt activation and high phosphorylation levels of the Akt targets FOXO1 and FOXO3a, which were maintained upon culture under low serum conditions (Supplementary Fig. S8A and S8B). Consistently, the *in vitro* proliferation of alveolar cells, similar to that of bronchiolar cells, was not decreased when the cells were grown in low (3% and 1.5%), compared to high (6% and 10%) serum concentrations for 1 week (Supplementary Fig. S8C). Knockdown of *ENTPD5* in alveolar cells did not restore sensitivity to serum (data not shown), indicating that *in vitro* culture of alveolar cells resulted in the activation of at least two distinct compensatory pathways leading to increased ENTPD5 expression, an enhancement of Akt activity, and resistance to serum. We therefore resorted to the use of KPTENp53 bronchiolar tumor cells to investigate the role of *ENTPD5* expression levels in modulating the sensitivity of *PTEN*-null tumors to DR.

To that end, we generated stable KPTENp53 bronchiolar tumor cell lines with *ENTPD5* (shE5-1 and shE5-2) or control *GFP* (shGFP) knockdown. Suppression of ENTPD5 resulted in a significant decrease in cellular N-glycosylation levels (Fig. 4C) and a decrease in IGF1Rβ levels that were accompanied by lower phosphorylation levels of Akt in cells cultured for 24 hours in media supplemented with insulin or IGF1 (Fig. 4D). We then asked whether a decrease in *ENTPD5* levels is sufficient to convert a DR-resistant *PTEN*-null tumor to one that is DR-sensitive. We had previously demonstrated that tumor cells with *in vivo* DR resistance exhibit *in vitro* constitutive Akt activation, despite serum starvation, and also proliferate in a growth-factor independent manner (2). Indeed, shGFP control bronchiolar tumor cells maintain constitutive activation of Akt when grown *in vitro* under low serum (3% and 1.5%), compared to high serum (10%) concentrations. Consistently, these cells display FOXO1 and FOXO3a phosphorylation levels that are maintained under low serum culture conditions (Fig. 4E and F).

Intriguingly however, compared to shGFP cells, the phosphorylation of Akt on S473 was higher in shE5-1 and shE5-2 cells grown in media supplemented with 10% serum (Fig. 4E and F and Supplementary Fig. S9A). The latter could be attributed to activation of compensatory pathways aiming at increasing Akt activity despite decreased ENTPD5 levels, although the precise mechanisms for such compensation remain unknown. Nevertheless, knockdown of *ENTPD5* resulted in decreased IGF1Rβ levels independent of serum, and a consistent and significant decrease in Akt phosphorylation under low serum conditions (3% and 1.5%). The Akt activity was mirrored by the phosphorylation pattern of its targets FOXO1/3a. Consistent with a recent report (8), we noticed induction of the ER stress markers BiP/GRP78 and CHOP/GADD153, as well as increased caspase-3 cleavage upon *ENTPD5* knockdown (Fig. 4E and F and Supplementary Fig. S9A). Moreover, proliferation of shE5-1 and shE5-2, but not that of shGFP cells was severely decreased when the cells were grown in low (3% and 1.5%), compared to high (6% and 10%) serum concentrations for 1 week (Figs. 5A and B and Supplementary Fig. S9B). Hence, knockdown of *ENTPD5* in *PTEN*-null bronchiolar cells results in decreased IGF1R levels and enhanced sensitivity of the tumor cells to low serum conditions *in vitro*. Similarly, knockdown of IGF1R in these cells resulted in decreased Akt activity, the induction of ER stress markers (albeit without

inducing caspase-3 cleavage) (Supplementary Fig. S10A and S10B) and decreased cellular proliferation, in response to low serum conditions (Supplementary Fig. S10C).

When transplanted subcutaneously in mice of the same strain (syngeneic transplants), shE5-1 tumors displayed larger volumes under *ad-libitum* conditions compared to shGFP controls (Fig. 5C). However, upon DR, which was initiated 1-2 days following tumor injection and maintained for 2 weeks, shE5-1 bronchiolar tumors, but not shGFP control tumors displayed a marked (~2-fold) decrease in tumor volume (Fig. 5C). This was accompanied by a significant 25% decrease in tumor cell proliferation in shE5-1, but not shGFP tumors, as measured by BrdU labeling (Fig. 5D). Consistent with the tissue culture results, higher levels of apoptosis (caspase-3 cleavage) were noted in shE5-1 compared to shGFP tumors, independent of the feeding regimen (Fig. 5E). Histological and immunohistochemical analyses of shGFP and shE5-1 transplant tumor sections revealed marked infiltration of tumor cells with *PTEN*-positive stroma, characterized by lower levels of ENTPD5 expression and Akt phosphorylation (S473), compared to adjacent *PTEN*-null tumor cells. Nevertheless, it was evident that the high Akt activity levels observed in *PTEN*-null tumor cells were significantly decreased upon *ENTPD5* knockdown under both *ad-libitum* and DR conditions (Fig. 5F). Suppression of ENTPD5 expression in the bronchiolar tumor cells therefore resulted in the conversion of *PTEN*-null tumors from DR-resistance to DR-sensitivity *in vivo*.

ENTPD5 Expression Modulates Akt activity and Sensitivity to DR in NSCLC

Our findings imply that loss of *PTEN* in a tumor model with low growth factor receptors does not necessarily result in Akt activation. In order to investigate this further in human samples, we analyzed the levels by immunohistochemistry, of PTEN, phospho-S473 Akt, ENTPD5 and epidermal growth factor receptor (EGFR) in 130 cases of lung adenocarcinoma, the most prevalent histologic subtype of NSCLC (19). Genetic alterations in *PTEN* are rare in NSCLC (20). However, decreased PTEN protein levels, partly attributed to promoter methylation (21), have been reported in 24% of cases. Consistently we find that out of 130 cases of human lung adenocarcinoma, 21% display low *PTEN* expression level. Interestingly, of the latter, 33% also harbor low p-S473 Akt activity levels. In all cases, phosphorylation of Akt on S473 positively correlates with *ENTPD5* expression (P=0.0011, Fisher test), as well as levels of EGFR (P=0.0013, Spearman r=0.247) (Fig. 6A-C).

A limited number of established NSCLC cell lines express low levels of PTEN, including NCI-H23, which harbors a nonsense mutation in exon 7 (22). We therefore characterized the sensitivity to serum *in vitro* of PTEN-low NCI-H23 cells, compared to that of A549 cells, which express high levels of PTEN (Fig. 7A-C). Unlike A549 cells, which display significantly decreased Akt activity upon serum starvation for 1 hour or 24 hours (compared to 10% serum conditions), NCI-H23 cells maintain similar Akt activity levels, in the presence or absence of serum (Fig. 7A and B). Moreover, A549 cells display a differential proliferation pattern when grown for 1 week, in increasing concentrations of insulin (1-1000ng/ml) or IGF-1 (0.5- 100ng/ml), whereas NCI-H23 cells proliferate to the same extent, independent of insulin or IGF1 levels (Fig. 7C). Knockdown of *ENTPD5* (shE5-a and shE5-b) in NCI-H23 cells resulted in a significant decrease in Akt activity when the cells were grown in media deprived of serum for 1 hour or 24 hours, compared to 10% serum conditions (Fig. 7D and E and Supplementary Fig. S11A and S11B). A similar effect was observed in A549 cells with stable knockdown of *ENTPD5* (Supplementary Fig. S11C and S11D), although significantly lower IGF1R (but not EGFR) levels were only observed under low (1.5%) serum conditions in both cell lines with *ENTPD5* knockdown (Fig. 7D and E and Supplementary Fig. S11A-S11D). Nevertheless, the proliferation of NCI-H23 cells with *ENTPD5* knockdown was significantly decreased when the cells were grown for 1

week under low insulin or IGF1 conditions compared to control NCI-H23-shGFP cells (Fig. 7F).

Discussion

Our results point to a heterogeneity of Akt activation in *PTEN*-null tumors of the same tissue. Furthermore, they confirm our previous findings that PI3K/Akt-activated tumors are resistant to DR. It is noteworthy that the alveolar and bronchiolar tumors that we studied in the KPTEN and KPTENp53 mice represent earlier tumor stages and that a distinct phenotype of Akt signaling and response to DR might prevail in later, more advanced stages. However, the heterogeneity in *PTEN* expression and Akt activity that we describe in the mouse can also be found in humans, within different cores of the same, relatively advanced, NSCLC adenocarcinoma cases (Fig. 6B and C). This is reminiscent of the recently reported intratumor heterogeneity detected by exome sequencing of clear cell carcinoma (23), and further underscores the challenges facing personalized medicine, including diagnosis and therapy. Studying the effect of *ENTPD5* expression on cellular Akt activity and sensitivity to DR in NSCLC was limited by the low availability of established NSCLC cell lines that are *PTEN*-null or express very low levels of PTEN (22), despite the previous report (21) and the evidence herein confirming that PTEN protein loss occurs in a significant portion (21-24%) of NSCLC cases. Although IGF1R but not EGFR levels were only decreased upon *ENTPD5* knockdown in the NCI-H23 NSCLC cell line under low serum conditions (Fig. 7D and E and Supplementary Fig. S11A and S11B), it is possible that the levels of other growth factor receptors were also affected in these cells. Nevertheless, we find that EGFR levels do correlate, in a positive manner with Akt phosphorylation and ENTPD5 expression in NSCLC adenocarcinoma cases (Fig. 6B and C).

Studying the KPTEN mouse has led us to describe a useful model and research tool, where adjacent tumors in the same tissue display differential signaling outputs and respond differently to metabolic status, despite sharing an identical genetic background. Either loss of *PTEN* alone (KPTEN alveolar cells) or high expression levels of *ENTPD5* and *IGF1R* (Kp53 and wild-type bronchiolar tumors) are not sufficient to drive high Akt activation. It is rather the concomitant loss of the PI3K antagonist (*PTEN*) and the presence of upstream positive activation of PI3K (through increased expression of *ENTPD5* and *IGF1R*) that resulted in Akt activation in the KPTEN bronchiolar tumor cells.

Unexpectedly, *ENTPD5* knockdown resulted in increased rather than decreased Akt activity in KPTENp53 bronchiolar cell lines grown in high (10%) serum conditions, compared to shGFP control cells (Fig. 4E and F, and Supplementary Fig. S9A). This was also observed in NCI-H23 NSCLC cells (Supplementary Fig. S11A and S11B). It is possible that the generation of cell lines with stable *ENTPD5* knockdown may have selected for cells with, or alternatively led to the compensatory induction of, Akt activation under high serum conditions. Nevertheless, *ENTPD5* suppression resulted in the conversion of the serum-resistant and DR-resistant KPTENp53 bronchiolar cells and NCI-H23 NSCLC cells to sensitivity to lower serum, insulin or IGF-1 conditions *in vitro* (Figs. 5A and B and 7F), and to DR *in vivo* (Fig. 5C). The induction of compensatory pathways favoring tumor cell growth upon loss of *ENTPD5* was consistent with the observation that transplanted KPTENp53 tumor cells with *ENTPD5* knockdown yielded tumors with larger volumes, compared to shGFP control tumors, when grown in *ad-libitum*-fed mice (Fig. 5C). It is noteworthy that an attempt to increase IGF1R protein levels (through lentiviral infection) in cells with *ENTPD5* knockdown was unsuccessful, despite significantly increasing IGF1R mRNA levels. In comparison, both protein and mRNA levels were increased in shGFP control cells stably overexpressing *IGF1R* (data not shown). It is possible that these results

underscore a key role for ENTPD5 in promoting the N-glycosylation, proper folding and stability of IGF1R proteins.

The intriguing observation that *ENTPD5* and *IGF1R* are expressed, at markedly higher levels in normal bronchiolar, versus alveolar cells (Fig. 2E, right panel) may be dependent upon the cell of origin of these two cell populations, and it remains to be determined what specific mechanisms underlie such differential *ENTPD5* and *IGF1R* expression in the same lung epithelial tissue. It is also possible that the alveolar and bronchiolar tumor cells described in the KPTEN and KPTENp53 mice are derived from different cells of origin in the lung. Bronchiolar tumors have indeed been found in a different mouse model of lung cancer to be more resistant to therapy (24). It is also interesting that *PTEN* loss in the mouse lung has not only been associated with an acceleration of *Kras*-driven tumorigenesis (12) but also an increase in the bronchioalveolar stem cell (BASC) pool (25, 26). Indeed, Yanagi et al. (25) reported a larger number of BASCs in an inducible mouse model of *PTEN* loss in SPC-expressing cells, leading to alveolar and bronchiolar hyperplasia, and susceptibility of developing spontaneous lung adenocarcinomas. Although Akt was shown to be activated in whole lysates of the tumor-bearing lungs, immunohistochemical staining was not performed, which would have potentially allowed for the detection of differential Akt activation in *PTEN*-null alveolar and bronchiolar tumor cells.

In sum, our studies point to a heterogeneity of Akt activation in the same *PTEN*-null tissue. Predicting the tumor response to systemic metabolic status, such as DR, or to anti-tumor therapies targeting PTEN/PI3K, needs therefore to be based upon Akt activity *per se*, rather than the genetic alterations in the PTEN/PI3K pathway.

Methods

Mouse studies

All animal studies and procedures were approved by the Animal Care and Use Committee at MIT and Boston Children's Hospital. Kp53 and KPTEN (129 svJae) mice were generated by crossing *LSL-Kras*^{G12D} (9) to either *p53*$^{fl/fl}$ (10) *or PTEN*$^{fl/fl}$ (11) mice, respectively. Kp53 and KPTEN progeny were intercrossed to generate KPTENp53 mice. Four- to eight-week old mice were infected by a single 67.5μl intranasal instillation of 3×10^7 infectious particles of adenovirus-Cre (University of Iowa), following isoflurane anesthesia (27). In syngeneic transplant experiments, 5- to 7-week-old donor KPTENp53 male mice were infected with adenovirus-Cre and tumors were allowed to grow for 4 weeks. Tumors were dissociated from donor lungs following euthanasia and subcutaneously injected (10^6 cells) in 4 to 5 month-old recipient KPTENp53 mice that were not infected with adenovirus-Cre. Recipient tumors were harvested 5 weeks following tumor cell injection. For bronchiolar tumor cell transplants, 10- to 14-week-old male KPTENp53 mice were injected with 10^6 tumor cells per injection. All subcutaneous cell injections were delivered in 100μl Hank's buffered salt solution (Invitrogen) with 15% phenol red-free, growth factor reduced Matrigel (BD Biosciences). For BrdU labeling experiments, BrdU (Sigma) was injected intraperitoneally (30 mg/Kg) 24 hours prior to euthanasia.

Dietary restriction

DR was performed as previously described (2). Mice were individually caged for at least 4 days prior to subdividing them into an AL-fed group (Prolab RMH 3000, 5P76) and a 40% DR group (LabDiet, 5B6V). Weekly body weights and food intake were recorded.

Necropsy and plasma analyses

Mice were euthanized at the beginning of the light cycle after retro-orbital blood withdrawal, and plasma was prepared as described (28). Plasma insulin and IGF1 were assayed using kits from CrystalChem and Diagnostic Systems Laboratories, respectively. Lungs and subcutaneous tumors were harvested and lung lobes were separated in ice cold PBS. Tissues were immediately fixed in formalin for later processing.

Cell dissociation and culture

Tumors from donor KPTENp53 mice (5 weeks following infection with adenovirus-Cre) were dissociated in HBSS (Invitrogen, Calcium/Magnesium free) containing 0.025% trypsin-EDTA (Invitrogen) and 1mg/ml collagenase IV (Worthington Biochemicals). Following a 2 hour-incubation with rotation at 37°C, the samples were quenched with a solution containing Leibovitz's L15 medium without phenol red (Invitrogen), 10mM Hepes pH 7.4 (Invitrogen), 1mg/ml bovine serum albumin (Sigma), 75U/ml DNaseI (Roche), and 100U/ml penicillin/streptomycin (Invitrogen). The cells were then pelleted, resuspended in 1 ml quench solution, and filtered through 40 μm cell strainers (BD Falcon). Cells were then either immediately injected subcutaneously into recipient mice, or seeded (10,000 to 40,000 cells/well) in 6-well plates for colony isolation. Using cloning cylinders (Corning), individual colonies were trypsinized from the parental cells and grown separately as either alveolar or bronchiolar cell lines depending on their expression of the alveolar marker SPC. Compared to parental cells, alveolar and bronchiolar cell lines were confirmed to be highly enriched in epithelial cells ($EpCAM^{hi}$) by flow cytometry analysis using an APC-conjugated CD326 (EpCAM) antibody (eBioscience, G8.8). For generation of mouse bronchiolar or human cells with stable *ENTPD5* and control *GFP* knockdown, lentiviral supernatants produced from pLKO.1 plasmids encoding the corresponding hairpins were used, and infected cells were selected for at least 7 days with 4μg/ml puromycin. Mouse ENTPD5 hairpins: shE5-1 (GTCCACATCTTGGGAAGAATA) and shE5-2 (CGCCTTCTACGCTTTCTCTTA); human ENTPD5 hairpins shE5-a (GCCCTGTTAAAGGATGGCTTT) and shE5-b (GCAGACTTGGTTTGAGGGTAT); control GFP hairpins: shGFP (CTACAACAGCCACAACGTCCT and TCTCGGCATGGACGAGCTGTA). Human non-small cancer cell lines A549 and NCI-H23 were obtained from American Type Culture Collection (ATCC; in 2006 and 2013, respectively); PC-9 cell line was a generous gift from Dr. Nabeel Bardeesy at MGH (2011); No authentication of A549 or PC-9 cells was done by the authors. ATCC cell lines are routinely authenticated by STR analysis (DNA profiling). All cells were grown in RPMI supplemented with 10% fetal bovine serum (FBS).

Cell Proliferation Assay

The assay was performed as previously described (2), using the proliferation kit II (XTT, Roche).

Immunoblotting and PHA blotting

Cells were rinsed once in ice-cold PBS and collected in lysis buffer containing 50 mM HEPES, pH 7.4, 40 mM NaCl, 2 mM EDTA, 50 mM NaF, 10 mM pyrophosphate, 10 mM glycerophosphate, EDTA-free protease inhibitors (Roche) and 1% Triton X-100. Proteins were resolved by 4–12% or 16% SDS–PAGE, and analyzed by immunoblotting as described (29) using antibodies for Akt (#4691), caspase-3 (#9662), BiP (#3177), CHOP (#5554), FOXO1 (#2880), IGF1Rβ (#3027), PTEN (#9552), phospho-S473 Akt (#4058) and phospho-T24/T32 FOXO1/3a (#9464) (1:1000, Cell Signaling Technology); ENTPD5 (#2997-1, 1:500, epitomics), SPC (#WRAB-9337, 1:5000, Seven Hills Bioreagents) and GAPDH (#sc-25778, 1:5000, Santa Cruz Biotechnology). For N-glycosylation assessment,

protein lysates were resolved by 10% SDS-PAGE and analyzed by blotting using HRP-conjugated PHA-E lectin (USBiological, #P3370-25).

Immunohistochemistry

Formalin-fixed lung lobes were bisected and embedded in paraffin. Paraffin-embedded lung or tumor sections were immunostained according to the manufacturers' protocols using antibodies for cleaved caspase-3 (#9664, 1:200), EGFR (#4267, 1:50), FOXO1 (#2880, 1:100), IGF1Rβ (#3027, 1:600), PTEN (#9559, 1:100) and phospho-S473 Akt (#4060, 1:50), from Cell Signaling Technology; SPC (#WRAB-9337, 1:15000, Seven Hills Bioreagents,); ENTPD5 (#2997-1, 1:5000, Epitomics), BrdU (#ab6326, 1:40, Abcam). For human samples, a pathologist scored, in a blinded fashion, the intensity of PTEN and p-S473 Akt staining in a first set of 130 lung adenocarcinoma cases on tissue microarray with 1-7 cores/case. Intensity scores ranged from 0 to 2, and represented none/weak (0), moderate (1) and strong staining (2). Correlations between p-Akt, ENTPD5 and EGFR were analyzed in a second set of 64 lung adenocarcinoma cases with 2- 8 cores/case. Scores for each tumor core were estimated using the following formula: Intensity score = 0 × (% area of tumor with weak staining) + 1 × (% tumor area with moderate staining) + 2 × (% tumor area with strong staining), where 200 would be the highest score. These scores were then converted to a binary system where values above "100" were converted to a score of "1" (high) and scores below 100 were converted to "0" (low). Use of human samples for immunostaining was approved by the Institutional Review Board at Massachusetts General Hospital (Protocol Number 2009P001838).

Tumor burden and BrdU quantification

Subcutaneous tumors were collected, their dimensions were measured with a caliper and tumor volume was estimated according to the ellipsoid formula (30). Lung tumor burden and BrdU labeling were quantified using cellSens software in either HE-stained or BrdU-stained, transversely sectioned lung lobes, respectively. Total bronchiolar or alveolar tumor area (distinguished by morphology) in each bisected lobe was measured and normalized to the corresponding lobe area. Values represent averages of whole lung tumor burden from at least 3 mice. The number of BrdU-positive cells per tumor area was quantified using cellSens software and averaged from 6-10 alveolar or bronchiolar tumors/lung of 3 mice, or from 3-7 areas (0.36 mm^2)/subcutaneous tumor in 3 mice.

Statistical analysis

Data are presented as means ± standard error of the mean (S.E.M.). In comparing two groups, a two-tailed non-paired Student's *t*-test was performed. For three or more groups, one-way ANOVA was performed, followed by a post hoc Student Newman-Keuls or Bonferroni test. Non-parametric two-tailed Fisher's exact test and Spearman correlation were performed for analysis of stain intensity scores. $P \leq 0.05$ (unless otherwise stated) was considered significant.

Supplementary Material

Refer to Web version on PubMed Central for supplementary material.

Acknowledgments

We thank F. Reinhardt, V. Gunduz and T. Zaytouni for assistance with experiments; H. Wu for the *PTEN*$^{fl/fl}$ mice and A. Berns for the *p53*$^{fl/fl}$ mice; X. Wang for *ENTPD5* constructs; R. Weinberg, members of the Sabatini and Kalaany laboratories and members of the Endocrinology Division at Boston Children's Hospital for support and discussions; R. Bronson for histological analysis; the Histology Core Facility at the Koch Institute for Integrative

Cancer Research and the Rodent Histopathology Core Facility at the Dana-Farber/Harvard Cancer Center for assistance with tissue sectioning and HE staining.

Grant Support This research was supported by the Anna Fuller Fund fellowship (N.Y. Kalaany); Boston Children's Hospital (N.Y. Kalaany, N.L. Curry, and V.O. Yilmaz), the Alexander and Margaret Stewart Trust Award (D.M. Sabatini); the David H. Koch Cancer Research Award (D.M. Sabatini) and NIH grants R01 AI04389, R01 CA129105 (D.M. Sabatini) and 2-P30-CA14051 (D.M Sabatini, T. Jacks and T.G. Oliver). D.M.S. is an investigator of the Howard Hughes Medical Institute.

References

1. Lee C, Longo VD. Fasting vs dietary restriction in cellular protection and cancer treatment: from model organisms to patients. Oncogene. 2011; 30:3305–16. [PubMed: 21516129]
2. Kalaany NY, Sabatini DM. Tumours with PI3K activation are resistant to dietary restriction. Nature. 2009; 458:725–31. [PubMed: 19279572]
3. Engelman JA, Luo J, Cantley LC. The evolution of phosphatidylinositol 3-kinases as regulators of growth and metabolism. Nat Rev Genet. 2006; 7:606–19. [PubMed: 16847462]
4. Stambolic V, Suzuki A, de la Pompa JL, Brothers GM, Mirtsos C, Sasaki T, et al. Negative regulation of PKB/Akt-dependent cell survival by the tumor suppressor PTEN. Cell. 1998; 95:29–39. [PubMed: 9778245]
5. Wu X, Senechal K, Neshat MS, Whang YE, Sawyers CL. The PTEN/MMAC1 tumor suppressor phosphatase functions as a negative regulator of the phosphoinositide 3- kinase/Akt pathway. Proc Natl Acad Sci U S A. 1998; 95:15587–91. [PubMed: 9861013]
6. Hollander MC, Blumenthal GM, Dennis PA. PTEN loss in the continuum of common cancers, rare syndromes and mouse models. Nat Rev Cancer. 2011; 11:289–301. [PubMed: 21430697]
7. Engelman JA. Targeting PI3K signalling in cancer: opportunities, challenges and limitations. Nat Rev Cancer. 2009; 9:550–62. [PubMed: 19629070]
8. Fang M, Shen Z, Huang S, Zhao L, Chen S, Mak TW, et al. The ER UDPase ENTPD5 promotes protein N-glycosylation, the Warburg effect, and proliferation in the PTEN pathway. Cell. 2010; 143:711–24. [PubMed: 21074248]
9. Jackson EL, Willis N, Mercer K, Bronson RT, Crowley D, Montoya R, et al. Analysis of lung tumor initiation and progression using conditional expression of oncogenic K-ras. Genes Dev. 2001; 15:3243–48. [PubMed: 11751630]
10. Jonkers J, Meuwissen R, van der Gulden H, Peterse H, van der Valk M, Berns A. Synergistic tumor suppressor activity of BRCA2 and p53 in a conditional mouse model for breast cancer. Nat Genet. 2001; 29:418–25. [PubMed: 11694875]
11. Lesche R, Groszer M, Gao J, Wang Y, Messing A, Sun H, et al. Cre/loxP-mediated inactivation of the murine Pten tumor suppressor gene. Genesis. 2002; 32:148–9. [PubMed: 11857804]
12. Iwanaga K, Yang Y, Raso MG, Ma L, Hanna AE, Thilaganathan N, et al. Pten inactivation accelerates oncogenic K-ras-initiated tumorigenesis in a mouse model of lung cancer. Cancer Res. 2008; 68:1119–27. [PubMed: 18281487]
13. Oliver TG, Mercer KL, Sayles LC, Burke JR, Mendus D, Lovejoy KS, et al. Chronic cisplatin treatment promotes enhanced damage repair and tumor progression in a mouse model of lung cancer. Genes Dev. 2010; 24:837–52. [PubMed: 20395368]
14. Keller A, Eistetter HR, Voss T, Schafer KP. The pulmonary surfactant protein C (SP-C) precursor is a type II transmembrane protein. Biochem J. 1991; 277:493–9. [PubMed: 1859376]
15. Calnan DR, Brunet A. The FoxO code. Oncogene. 2008; 27:2276–88. [PubMed: 18391970]
16. Serrano M, Blasco MA. Putting the stress on senescence. Curr Opin Cell Biol. 2001; 13:748–53. [PubMed: 11698192]
17. Lowe SW, Cepero E, Evan G. Intrinsic tumour suppression. Nature. 2004; 432:307–15. [PubMed: 15549092]
18. Trombetta ES, Helenius A. Glycoprotein reglucosylation and nucleotide sugar utilization in the secretory pathway: identification of a nucleoside diphosphatase in the endoplasmic reticulum. Embo J. 1999; 18:3282–92. [PubMed: 10369669]

19. Colby, TV.; Koss, M.; Travis, WD. Adenocarcinoma of the lung. In: Rosai, J.; Sobin, LH., editors. Atlas of Tumor Pathology: Tumors of the lower respiratory tract. Armed Forces Institute of Pathology; Washington, DC: 1995. p. 179-201.
20. Ding L, Getz G, Wheeler DA, Mardis ER, McLellan MD, Cibulskis K, et al. Somatic mutations affect key pathways in lung adenocarcinoma. Nature. 2008; 455:1069–75. [PubMed: 18948947]
21. Soria JC, Lee HY, Lee JI, Wang L, Issa JP, Kemp BL, et al. Lack of PTEN expression in non-small cell lung cancer could be related to promoter methylation. Clin Cancer Res. 2002; 8:1178–84. [PubMed: 12006535]
22. Forgacs E, Biesterveld EJ, Sekido Y, Fong K, Muneer S, Wistuba II, et al. Mutation analysis of the PTEN/MMAC1 gene in lung cancer. Oncogene. 1998; 17:1557–65. [PubMed: 9794233]
23. Gerlinger M, Rowan AJ, Horswell S, Larkin J, Endesfelder D, Gronroos E, et al. Intratumor heterogeneity and branched evolution revealed by multiregion sequencing. N Engl J Med. 2012; 366:883–92. [PubMed: 22397650]
24. Li D, Shimamura T, Ji H, Chen L, Haringsma HJ, McNamara K, et al. Bronchial and peripheral murine lung carcinomas induced by T790M-L858R mutant EGFR respond to HKI-272 and rapamycin combination therapy. Cancer Cell. 2007; 12:81–93. [PubMed: 17613438]
25. Yanagi S, Kishimoto H, Kawahara K, Sasaki T, Sasaki M, Nishio M, et al. Pten controls lung morphogenesis, bronchioalveolar stem cells, and onset of lung adenocarcinomas in mice. J Clin Invest. 2007; 117:2929–40. [PubMed: 17909629]
26. Tiozzo C, De Langhe S, Yu M, Londhe VA, Carraro G, Li M, et al. Deletion of Pten expands lung epithelial progenitor pools and confers resistance to airway injury. Am J Respir Crit Care Med. 2009; 180:701–12. [PubMed: 19574443]
27. DuPage M, Dooley AL, Jacks T. Conditional mouse lung cancer models using adenoviral or lentiviral delivery of Cre recombinase. Nat Protoc. 2009; 4:1064–72. [PubMed: 19561589]
28. Kalaany NY, Gauthier KC, Zavacki AM, Mammen PP, Kitazume T, Peterson JA, et al. LXRs regulate the balance between fat storage and oxidation. Cell Metab. 2005; 1:231–44. [PubMed: 16054068]
29. Kim DH, Sarbassov DD, Ali SM, King JE, Latek RR, Erdjument-Bromage H, et al. mTOR interacts with raptor to form a nutrient-sensitive complex that signals to the cell growth machinery. Cell. 2002; 110:163–75. [PubMed: 12150925]
30. Wapnir IL, Wartenberg DE, Greco RS. Three dimensional staging of breast cancer. Breast Cancer Res Treat. 1996; 41:15–19. [PubMed: 8932872]

Significance

Our studies point to a heterogeneity of Akt activation in the same murine *PTEN*-null lung tissue and in human NSCLC, further underscoring the challenges facing personalized cancer therapy based solely on cancer genotype. Our findings therefore indicate that the tumor response to anti-cancer therapies, including DR, needs to be based upon PI3K/Akt activity *per se*, rather than genetic alterations in the PTEN/PI3K pathway.

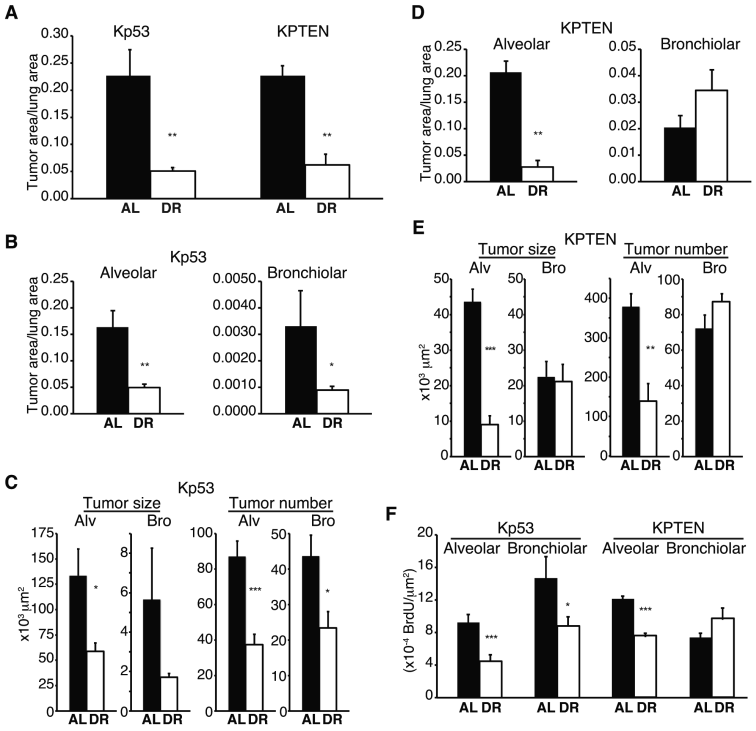

Figure 1. *PTEN*-null bronchiolar but not alveolar tumors in a *Kras*-driven mouse model of lung cancer are resistant to DR

A, Total tumor burden, measured by the ratio of tumor area over lung area in Kp53 and KPTEN mice that have been either *ad libitum*-fed (AL) or dietary restricted (DR) for 3 weeks (n=3-5 mice). **B** and **D**, Alveolar and bronchiolar tumor burden quantified, respectively, in lungs of Kp53 (**B**) or KPTEN (**D**) mice described in (**A**). **C** and **E**, Average size (left panels) and average number (right panels) of distinct alveolar (alv) or bronchiolar (bro) tumors in Kp53 (**C**) or KPTEN (**E**) mice, described in (**A**). **F**, Tumor cell proliferation measured by BrdU incorporation in alveolar and bronchiolar tumor cells of Kp53 and KPTEN mice described in (**A**) (n=6-10 tumors in 2-3 mice). Data are means ± S.E.M.; $*P \leq 0.05$; $**P \leq 0.01$; $***P \leq 0.001$. ANOVA followed by Newman-Keuls test was applied in (**A**) and Student's *t*-test in (**B-F**).

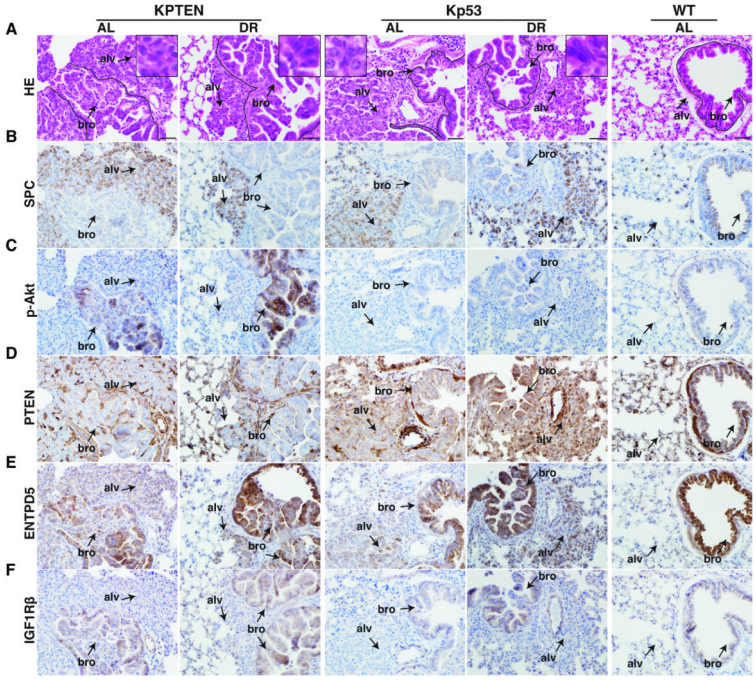

Figure 2. *PTEN*-null bronchiolar but not alveolar tumors display high Akt activation and express high levels of ENTPD5 and IGF1R

A-F, H&E staining (**A**) and immunohistochemical analyses of SPC (**B**), phospho-S473 Akt (**C**), PTEN (**D**), ENTPD5 (**E**) and IGF1Rβ (**F**) in sequential sections of lungs from KPTEN mice under AL or DR conditions and from an AL-fed wild-type mouse (WT). Arrows indicate alveolar (alv) or bronchiolar (bro) tumors. All pictures were captured under the same magnification; scale bars, 40μm. Framed insets in (**A**) are a 4-fold magnification of representative alveolar (AL panels) or bronchiolar (DR panels) tumor areas of corresponding H&E larger images. The black line in (**A**) marks the outside layer of tumor-enclosing (KPTEN, Kp53) or normal (WT) bronchioles.

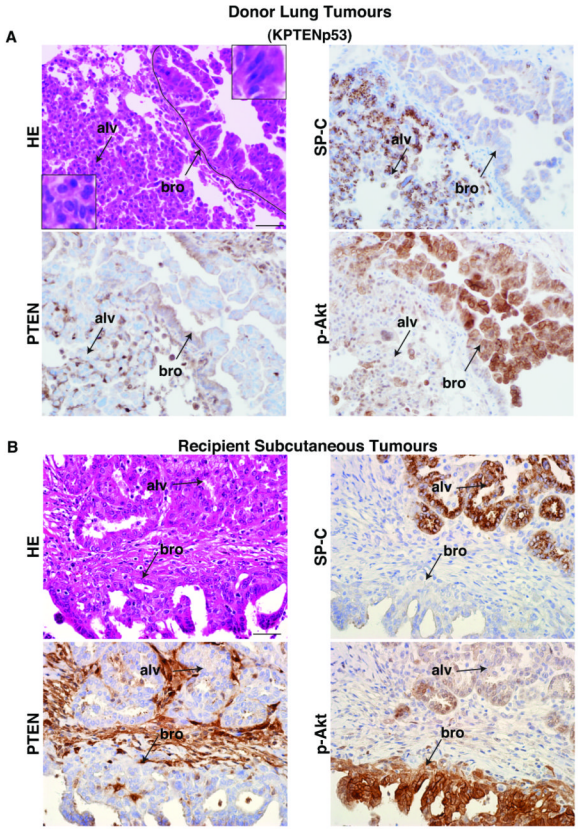

Figure 3. The alveolar tumor phenotype of low Akt activity despite *PTEN* loss is maintained upon transplantation from donor to recipient mice

A and **B**, H&E staining and immunohistochemical analyses of SPC, PTEN, and phospho-S473 Akt, in the lungs of a KPTENp53 donor mouse (**A**) and in subcutaneous tumors of a recipient KPTENp53 mouse, 5 weeks following injection of the donor tumor cells (**B**). Arrows indicate alveolar (alv) or bronchiolar (bro) tumors. All pictures were captured under the same magnification; scale bars, 40μm. Framed insets in (**A**) are a 3-fold magnification of a representative alveolar (lower left) or bronchiolar (upper right) tumor area of the H&E larger image. The black line in (**A**) (left panel) marks the outside layer of a tumor-enclosing bronchiole.

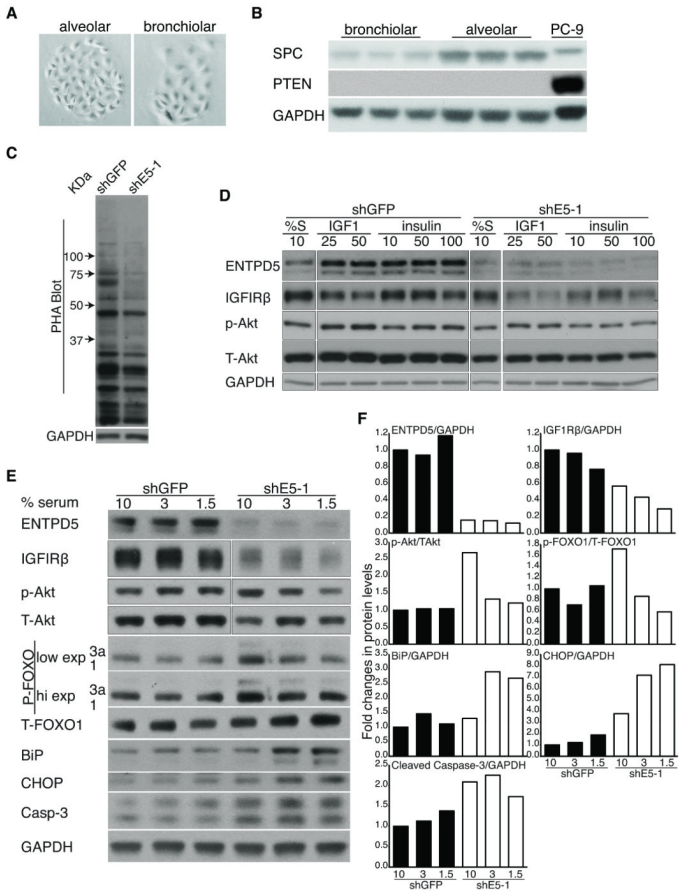

Figure 4. ENTPD5 modulates growth factor receptor levels and Akt activity in *PTEN*-null tumor cells

A, Representative pictures of KPTENp53 tumor cell colonies (10× magnification). **B**, SPC, PTEN and GAPDH protein levels in KPTENp53 cells compared to NSCLC PC-9 cells. **C**, N-glycosylation levels in bronchiolar KPTENp53 cell lines with stable knockdown of control *GFP* (shGFP) or *ENTPD5* (shE5-1), as assessed by PHA-E lectin blotting. GAPDH protein levels are represented as a loading control. **D**, Levels of ENTPD5, IGF1Rβ, phospho-S473 Akt, total Akt and GAPDH in shGFP and shE5-1 cells grown for 24 hours in media supplemented with 10% serum (S) or with different concentrations of IGF1 (25 or 50 ng/ml) or insulin (10, 50 or 100 ng/ml), in the absence of serum. **E**, ENTPD5, IGF1Rβ, phospho-S473 Akt, total Akt, phospho-T24/T32 FOXO1/3a (p-FOXO1/3a, low and high exposure levels), total FOXO1, BiP, CHOP, cleaved capase-3 (casp-3) and GAPDH protein levels in shGFP and shE5-1 cells described in (**C**), grown in the presence of 10%, 3% or 1.5% serum for 72 hours. **F**, Graphs representing quantified changes (obtained by ImageJ) in p-Akt/T-Akt, p-FOXO1/T-FOXO1, or ENTPD5, IGF1Rβ, BiP, CHOP cleaved caspase-3, over GAPDH protein levels assayed for in (**E**). (**C**-**F**) are representative of at least three independent experiments. In (**D**) and (**E**), separated lanes of individual blots were acquired from a single electrophoresis gel.

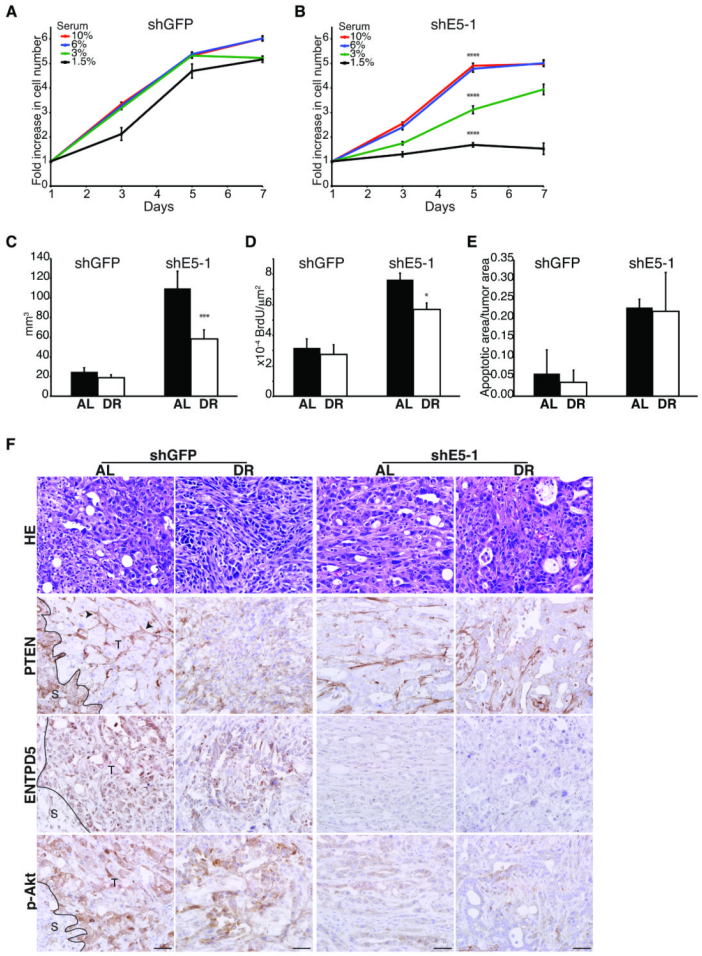

Figure 5. *ENTPD5* modulates *PTEN*-null tumor sensitivity to serum *in vitro* and DR *in vivo*

A and **B**, Proliferation curves of bronchiolar KPTENp53 cell lines with stable knockdown of control *GFP* (shGFP) or *ENTPD5* (shE5-1), grown in the presence of 10%, 6%, 3% or 1.5% serum for 7 days (n=6). **C**, Volumes of shGFP or shE5-1 bronchiolar KPTENp53 subcutaneous tumor transplants in AL or DR mice, as estimated by the ellipsoid formula (30) (n=10-12). **D**, Proliferative indices of tumors measured by BrdU labeling quantification in shGFP and shE5-1 tumor transplants described in (**C**). **E**, Apoptotic indices represented as apoptotic area/total tumor area in shGFP and shE5-1 tumor transplants described in (**C**) and assessed by immunohistochemical analysis of cleaved caspase-3 (n=4 mice/condition). **F**, H&E staining and immunohistochemical analyses of PTEN, ENTPD5 and phospho-S473 Akt in sequential sections of tumor transplants described in (**C**). All pictures were captured under the same magnification; scale bars, 40μm. In (**A-E**), data are means ± S.E.M; *$P <$ 0.05; ***$P < 0.001$; ****$P < 0.0001$ (ANOVA/Bonferroni tests for differences between 10%, 3% and 1.5% serum at day 5 in (**A** and **B)** or Newman-Keuls test in (**C-E**)). (**A** and **B)** are representative of at least three, and (**C-F**) of two independent experiments, respectively. The black line in (**F**) (left panel) separates predominantly stromal “S” areas from tumor “T” areas.

A

Cases of Human NSCLC	130	
PTEN Low	27/130	21%
PTEN Low/p-Akt low	9/27	33%

		ENTPD5 high	ENTPD5 low
p-Akt	high	13	5
	low	4	19

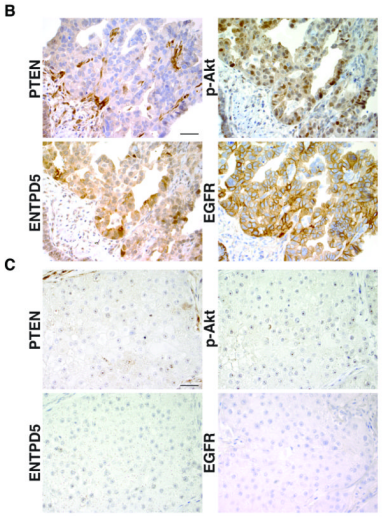

Figure 6. ENTPD5 expression correlates with EGFR and activated Akt levels in human NSCLC

A, Percentages of *PTEN*-low lung adenocarcinoma cases with at least one core scoring either “high” or “low” for p-S473 Akt; Fisher test illustrating the correlation between ENTPD5 and p-Akt ($P < 0.0011$). **B** and **C**, Immunohistochemistry of *PTEN*-low adenocarcinoma cases with high (**B**) or low (**C**) p-S473 Akt, ENTPD5 and EGFR levels. All pictures were captured under the same magnification; scale bars, 40μm.

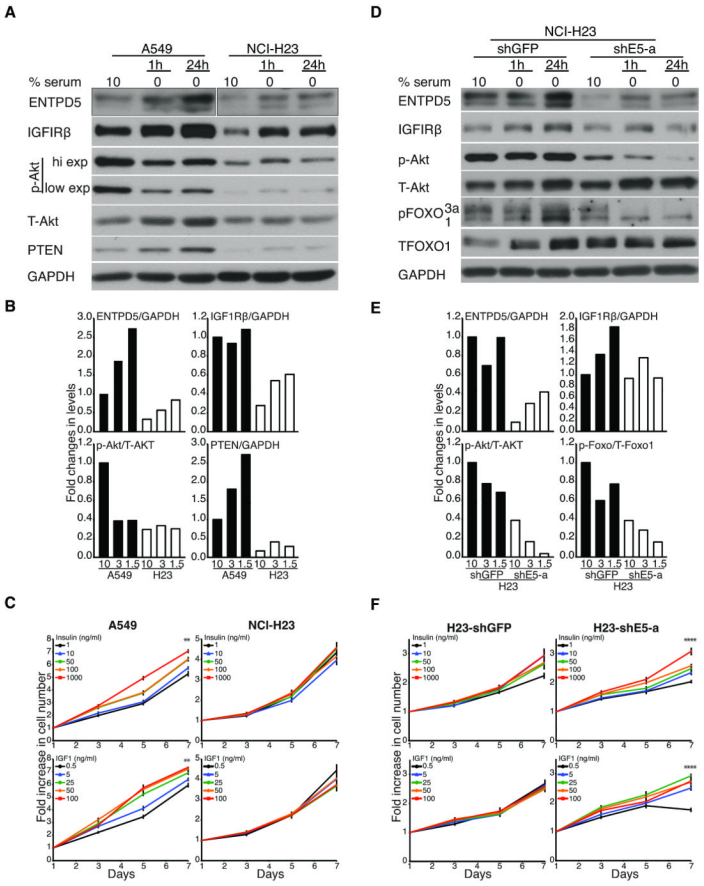

Figure 7. Suppression of ENTPD5 in human NSCLC cells results in decreased Akt activity and decreased proliferation under low serum conditions

A and **D**, Levels of ENTPD5, IGF1Rβ, phospho-S473 Akt (high and low exposures), total Akt, PTEN, and GAPDH in A549 and NCI-H23 human NSCLC cell lines (**A**), or in NCI-H23 cells with stable knockdown of *GFP* or *ENTPD5* (shE5-a) (**D**), grown in media supplemented with 10% serum, or 0% serum for 1 or 24 hours. **B** and **E**, Graphs representing quantified changes (obtained by ImageJ) in ENTPD5, IGF1Rβ, or PTEN, over GAPDH protein levels or p-Akt/T-Akt, assayed for in (**A**) or (**D**), respectively. **C** and **F**, Proliferation curves of A549 and NCI-H23 (**C**), described in (**A**) or NCI-H23-shGFP, NCI-H23-shE5-a cell lines (**F**), described in (**D**), grown in the presence of 0.1% serum supplemented with increasing concentrations of insulin or IGF1 for 7 days (n=6). $^{**}P < 0.01$; $^{****}P < 0.0001$ (ANOVA/Bonferroni tests for differences between 1ng/ml insulin or 0.5ng/ml IGF1 and all other conditions at day 7 in (**C** and **F**)). In (**A**) separated lanes of the ENTPD5 blot were acquired from a single electrophoresis gel.